

*Presented at the Human Factors Issues in Combat Identification Workshop, Gold Canyon, Arizona, May 13, 2008.*

## **WHAT VISUAL DISCRIMINATION OF FRACTAL TEXTURES CAN TELL US ABOUT DISCRIMINATION OF CAMOUFLAGED TARGETS**

Vincent A. Billock  
General Dynamics Advanced Information Systems

Douglas W. Cunningham  
University of Tübingen

Brian H. Tsou  
U.S. Air Force Research Laboratory

### **Abstract**

Most natural images have  $1/f^\beta$  Fourier image statistics, a signature which is mimicked by fractals and which forms the basis for recent applications of fractals to camouflage. To distinguish a fractal camouflaged target (with  $1/f^{\beta^*}$  statistics) from a  $1/f^\beta$  natural background (or another target), the exponents of target and background (or other target) must differ by a critical amount ( $d\beta = \beta - \beta^*$ ), which varies depending on experimental circumstances. The same constraint applies for discriminating between friendly and enemy camouflaged targets. Here, we present data for discrimination of both static and dynamic fractal images, and data on how discrimination varies as a function of experimental methods and circumstances. The discrimination function has a shallow minimum near  $\beta = 1.6$ , which typifies images with less high spatial frequency content than the vast majority of natural images ( $\beta$  near 1.1). This implies that discrimination between fractal camouflaged objects is somewhat more difficult when the camouflaged objects are sufficiently similar in statistics to the statistics of natural images (as any sensible camouflage scheme should be), compared to the less natural  $\beta$  value of 1.6. This applies regardless of the  $\beta$  value of the background, which has implications for fratricide; friendlies and hostiles will be somewhat harder to tell apart for naturalistically camouflaged images, even when friendlies and hostiles are both visible against their backgrounds. The situation is even more perverse for “active camouflage”. Because of perceptual system nonlinearities (stochastic resonance), addition of dynamic noise to targets can actually enhance target detection and identification under some conditions.

**APPROVED FOR PUBLIC RELEASE**

## Introduction

Discrimination tasks in combat target identification are legion. For example, operators need to discriminate a target against a background and to discriminate a set of similar targets from one another. The first task is a necessary, but not sufficient condition for targeting, while the second task is essential to solve decoy and friendly-fire problems. Both tasks are complicated by camouflage. If it were necessary to consider the set of all possible targets, backgrounds and camouflage, the combinatorial problem would be disheartening. However, a consideration of visual psychophysics, image science and fractal mathematics suggests that a particularly simple optical signature provides a low-dimensional solution.

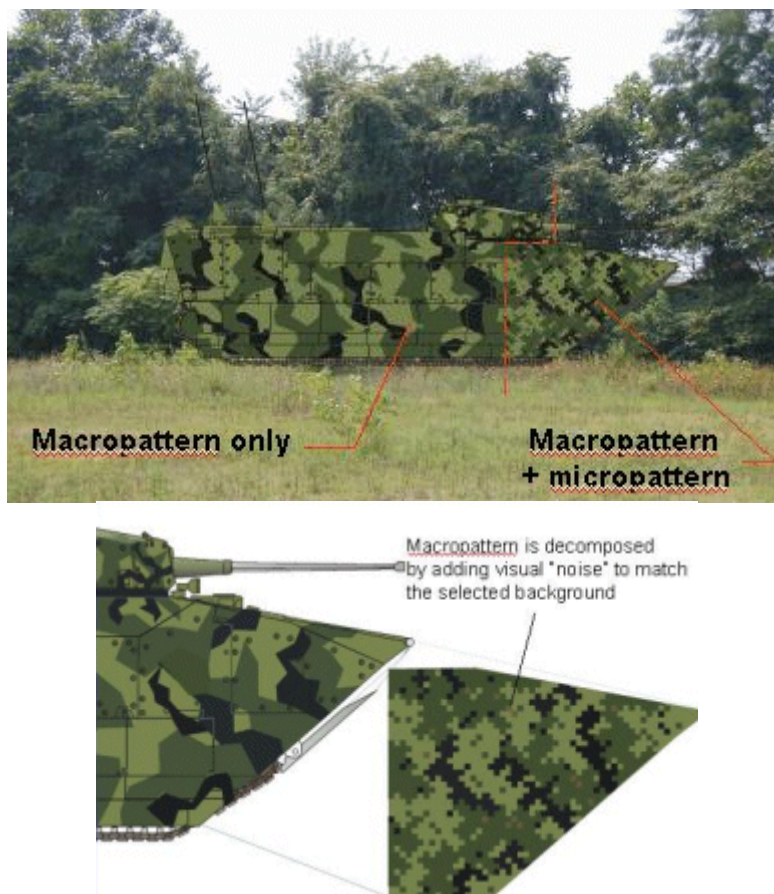


**Figure 1.** An Expeditionary Fighting Vehicle (General Dynamics, Inc.) concealed against foliage with two different camouflage schemes. The rear of the vehicle is in standard single-scale NATO camouflage and pops-out from the foliage background. The front of the vehicle (see figure bottom) is concealed by a two-scale MARPAT camouflage pattern and is less conspicuous (O'Neill et al., 2004). If the number of scales increases, the perception of fractal-like camouflage is less distance dependent. Courtesy of the United States Marine Corps Systems Command.

### Background: Perceptual Popout, Fractals and Camouflage

It is well known that humans effortlessly (and preattentively) discriminate images which differ significantly in their second-order statistics (the so-called "pop-out" phenomenon), while images

that have similar second-order statistics must usually be compared on a more laborious point-by-point basis (Julesz & Caelli, 1979; Caelli, 1981). Most natural (and many artificial) images have surprisingly regular  $1/f^\beta$  Fourier spatial amplitude spectra (Table 1; see Field & Brady, 1997 and Billock, 2000 for review), a signature which is mimicked by random fractals and which forms the basis for fractal forgeries (Voss, 1985) and digital camouflage. The exponent  $\beta$  (the slope of the Fourier spectra when plotted on log-log coordinates) is a second-order statistic. A growing body of evidence suggests that humans are adapted to this statistical regularity in the environment and that this evolutionary/developmental adaptation forms the basis for neural image enhancement and deblurring (Billock, 2000; Billock et al., 2001a,b; Campbell et al., 1978; Hammett & Bex, 1996). A hallmark of random fractal images is the presence of statistically similar features at every spatial scale. The lawful relationship between spatial scales is termed self-similarity and is one of the properties of natural images that give rise to  $1/f^\beta$  spectra. This property is what enables random fractals to mimic natural images and backgrounds. For example, a tree branch gives rise to several smaller branches, which give rise to many twigs – a random fractal that distributes and scales its features similarly can emulate foliage and act as camouflage. The  $\beta$  value (or equivalently, fractal dimension) is often used as a mathematical measure of image texture and its perceptual correlates (Cutting & Garvin, 1987; Kumar et al., 1993; Pentland, 1988; Rogowitz & Voss, 1990; Taylor et al., 2005). It follows that some aspects of fractal image discrimination can emulate natural image discrimination (Hansen & Hess, 2006; Thomson & Foster, 1997; Parraga & Tolhurst, 2000; Tolhurst & Tadmor, 2000).

*Table 1. Second-order statistics of natural images*

Study	Number of images	$\beta \pm 1sd$
Burton & Morehead (1987)	19	1.05 $\pm$ .12
Field & Brady (1997)	20	1.10 $\pm$ 0.14
Parraga (1998)	29	1.11 $\pm$ 0.13
Ruderman (1994)	45	0.905
Webster & Miyahara (1997)	48	1.13
Thomson & Foster (1997)	82	1.19
Field (1993)	85	1.10
van Hateren (1992)	117	1.065 $\pm$ .18
Tolhurst et al. (1992)	135	1.20 $\pm$ .13
Schaaf & Hateren (1996)	276	0.94 $\pm$ 0.21
Dong & Atick (1995)	320	1.15
Weighted average	1176	1.08

If natural backgrounds are fractal-like, camouflage should be designed along similar principles. Newer camouflage schemes like MARPAT (U.S Marines) and CADPAT (Canadian Armed Forces) use a two-scale scheme which is noticeably better at blending into terrain and foliage than the older single-scale schemes. For example, detection times for MARPAT (Fig. 1) camouflaged targets are about 2.5 times longer than detection of NATO single-scale camouflage

and recognition times following detection increase by an additional 20% (O'Neill et al., 2004). Some newer camouflage schemes – inspired by fractals – have more than two scales. (True fractal camouflage would be defined by statistical similarity at every visible spatial scale, but limited size and printing resolution result in a restricted range of scales.) More complicated schemes are possible, including the use of multi-fractals which mimic blends of particular textures that occur in natural images (e.g., plant growth on fractured rock). Here, we study human abilities to discriminate images based on small differences in the  $\beta$  signature and place the results in context with camouflage and with earlier texture discrimination studies.

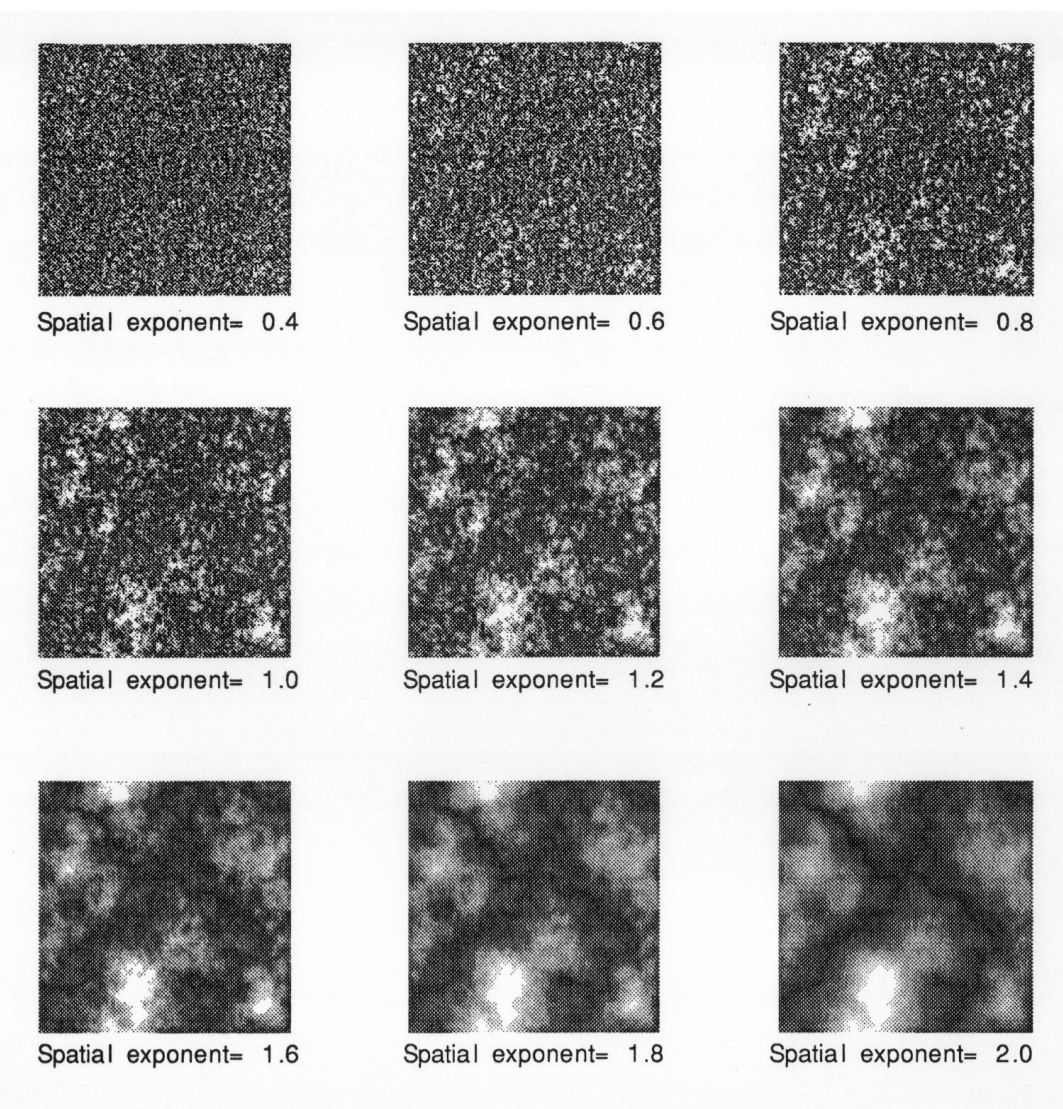


**Figure 2.** Fractal textures like those used in the experiments. Each fractal in this figure has  $1/f^\beta$  amplitude spectrum and identical phase spectra, and is synthesized by spatial frequency filtering the same set of random gray levels. The lack of weight in the higher spatial frequencies can easily be seen in the coarseness of the images as the exponent  $\beta$  increases.

## Methods

### *Participants*

The four observers were all myopes corrected to at least 20/20 binocular acuity. All are professional psychophysicists and highly experienced observers, with prior work in the psychophysics of "white" and "colored" (spatiotemporally non-uniform) visual noise. One subject (SF) was naïve to the purpose of the experiment. Another subject (VB) has a diagnosed, mild, congenital visual condition – optic nerve hypoplasia (a low density of neurons in the optic nerve). Although his vision is considered normal by standard clinical measures (including acuity), his contrast sensitivity is slightly depressed (about 1 sd) at all spatial frequencies relative to a large sample of age-matched-normals; this depression in sensitivity is worse for higher spatial frequencies. His vision is relevant here because it provides us a gauge of the effects of spatial under-sampling in an otherwise intact visual system.

### *Apparatus*

All stimuli were generated and presented on a Silicon Graphics O<sub>2</sub> graphics workstation with a linearized 30 Hz display. Stimuli were viewed binocularly with natural pupils in a well-lit room (ambient luminance in the plane of the monitor was 3.5 cd/m<sup>2</sup>). Subjects were comfortably fixed in place by a chin rest at two viewing distances, 40 cm and 100 cm. The far distance was a limiting case (e.g., each pixel subtends 0.016 deg at 100 cm, matching the subjects' 1 arc min spatial resolution). The stimuli consisted of static, grayscale, random-phase fractals (e.g., Fig. 2) whose Fourier amplitude spectra were described by

$$A(f_s) = kf_s^{-\beta} \quad \text{Eq. 1}$$

Where  $k$  is a constant and  $f_s$  is spatial frequency. (In visual psychophysics, amplitude rather than power spectra are used, because amplitude is proportional to perceptual contrast for each spatial frequency component.) For each stimulus, the average luminance was constant at 8.57 cd/m<sup>2</sup> and the Root Mean Square Contrast (a good measure of perceptual contrast for noise-like textures; Moulden *et al.*, 1990; Peli, 1990, 1997) was 10.98%. For consistency with another study, each fractal contained 64x64 pixels (18x18mm). Thus, at 40 cm, the stimuli subtended 2.58<sup>o</sup> embedded in a 43.9<sup>o</sup> horizontal by 36.4<sup>o</sup> vertical dark surround. At 100 cm, each stimulus subtended 1.03<sup>o</sup> embedded in a 21.1<sup>o</sup> horizontal by 16.4<sup>o</sup> vertical dark surround. Both a reference and a comparison image were generated for each trial. The images were created by filling a 64X64 array with random white noise (256 gray-levels). This white-noise image was Fourier-transformed and the amplitudes of all spatial frequencies were equalized to ensure that the noise was uniformly flat. The resulting amplitude spectra were filtered so that they followed a power law relationship (Eq. 1), and then inverse-Fourier transformed to produce the stimuli.

### *Procedure*

Just noticeable discrimination thresholds (79% correct criterion) for fractal spatial exponents were measured using a two-alternative forced-choice adaptive staircase procedure with a 1 db step size (MacMillan & Creelman, 1991). Ten  $\beta$  exponents were used (0.4, 0.6, 0.8, 1.0, 1.2, 1.4, 1.6, 1.8, 2.0, and 2.2) for the reference images. For the comparison image, the fractal exponent was equal to the exponent,  $\beta$ , of its reference image plus a small increment,  $\Delta\beta$ . Observers were asked to identify the image with the lower spectral exponent, and were provided with immediate

feedback on the accuracy of their response. If the observer correctly identified the reference image three times in a row, the difference between the two images' exponents  $\Delta\beta$  was decreased. In contrast,  $\Delta\beta$  was increased after each incorrect response. Each staircase continued for 8 reversals, with the mean of the last 6 reversals being used as a measure of the threshold. Two presentation conditions (Sequential and Simultaneous) were used. In the Simultaneous condition, the reference and comparison stimuli were presented side by side (1.1 mm apart) for 2.133 seconds. The location of the reference image (left versus right) was randomized across trials. In the Sequential condition, the two stimulus images were sequentially presented in the center of the screen for 2.133 seconds each. The screen was blanked for 500 ms between the two images to prevent masking effects. The order of presentation of the reference and comparison images was randomized across trials. Combining two viewing distances with two presentation modes yielded four experimental conditions. Two observers were presented with the Near conditions first, and two with the Far conditions first. For all observers, the presentation style (simultaneous vs. sequential) alternated after each threshold. The order of presentation of the 10 exponents was randomized for each of the 4 conditions. Each threshold was measured 3 times, with the thresholds in all 4 conditions being completed once before being re-measured. This required approximately 20 hours of data collection per subject, which was generally completed in 2 one-hour sessions each day, over a two-week period.

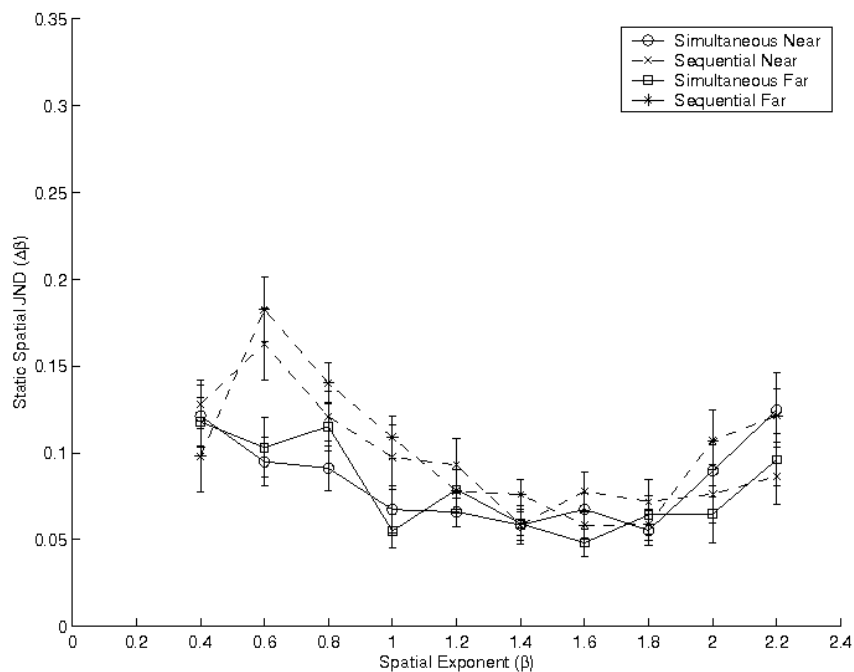


*Figure 3. Group averages for all 4 conditions.*

## Results and Analysis

### *General Findings*

Discrimination thresholds ( $d\beta$ ) are generally in the range of 0.05-0.20 for  $\beta$  values of 0.4-2.2 (see Figs. 3, 4). The discrimination function is not flat; it has higher (worse) discrimination thresholds for both low and high values of  $\beta$ , and lower (better) discrimination thresholds for in-between

values of  $B$ . The minimum is near  $\beta=1.6$ , which typifies images with less high spatial frequency content than the vast majority of natural images ( $\beta$  near 1.1). This implies that discrimination between fractal camouflaged objects is somewhat more difficult when the statistics of camouflaged objects are sufficiently similar to the statistics of natural images (as any sensible camouflage scheme should be), compared to the less natural  $B$  value of 1.6. This applies regardless of the background's  $\beta$  value, which has implications for fratricide; friendlies and hostiles will be somewhat harder to tell apart for naturalistically camouflaged images, even when friendlies and hostiles are both visible against their backgrounds.

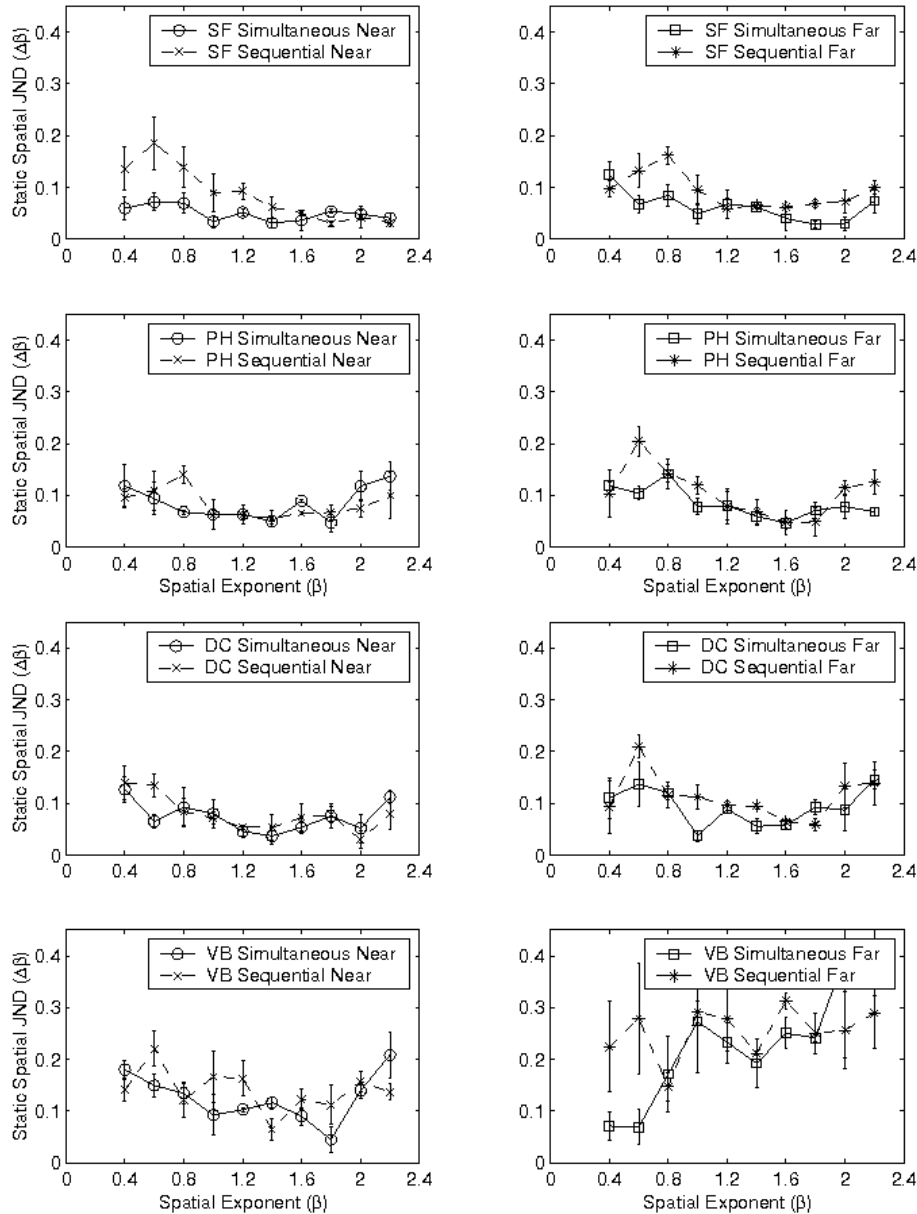


Figure 4. Individual data from all 4 observers for all 4 conditions.

### ***Effect of Viewing Distance***

For ideal 1/f images, there should be little effect of viewing distance, because increasing viewing distance would simply shift a lower spatial frequency component into a higher spatial frequency, but the relationship between the spatial frequencies would be preserved. However, all physically obtainable fractals are limited to a range of spatial scales set at the lower end by the size of the image and at the upper end by the size of the pixels. Shifting the viewing distance from 40 to 100 cm therefore shifts the spatial frequency range of the fractal image by a factor of 2.5, but no information is lost because the stimuli were designed so that the individual pixels were resolvable at the far viewing distance by all observers. Accordingly, for three of the observers (DC, PH, and SF), viewing distance had little effect, although there is a slight trend suggesting lower thresholds in the nearer viewing distances (see Figure 4a-c). For VB, however, the Far thresholds (and their variability) were noticeably elevated compared to either his Near thresholds or to the other observers' Far thresholds (see Fig. 4). VB's anomalous results may be due to sampling problems induced by a mild congenital defect – a developmental paucity of retinal ganglion cells (optic nerve hypoplasia). Electrophysiological studies in VB and other hypoplastic subjects and post-mortem histology in other hypoplastics indicate that both retinal pre-processing and cortical post-processing seem to be normal (Billock et al., 1994) and point to reduction in retinal ganglion cell numbers as the sole cause of abnormal vision in hypoplasia. In the case of VB, perimetric thresholds are flattened relative to normals, suggesting the subject did not gain a full measure of the elevated density of foveal ganglion cells that develops in normals. Since pixel size and stimulus size are fixed, any sampling problems would more likely manifest as a threshold elevation at the far viewing conditions. Moreover, if the reduced sampling is not homogeneous, then this could increase variability (because, from trial to trial, filtered noise features would fall on neighboring retinal locations with different retinal sampling densities).

### ***Effect of Presentation Style***

Simultaneous viewing simulates the task of making a side-by-side comparison of fractal camouflaged targets, while sequential viewing simulates the task of comparing a target to one that is in memory; in theory and experiment the two paradigms can lead to somewhat different results (Garcia-Perez *et al.*, 2005; Hansen & Hess, 2006). The discrimination function is similar for both conditions (Figs. 3 and 4) but there is a small advantage for simultaneously-viewed images, relative to sequentially-viewed ones, especially for small values of  $\beta$ . This tendency can be clearly seen when the data from the 4 subjects are pooled (Fig. 3). This is contrary to Hansen & Hess (2006), who found an advantage for sequential viewing, and attributed differences between the two conditions to differences in the portions of retina they cover. However, our near-sequential and far-simultaneous stimuli covered very similar regions of central retina (2.6° and 2.3° respectively), and yet simultaneous viewing yielded lower thresholds for nine of ten exponents (and tied for the tenth). This suggests that for our experiment, the memory demands of sequential viewing were disadvantageous, a design consideration for combat target displays.

## **Discussion**

### ***Comparison to Related Studies: Static Fractals***

Some prior studies of fractal discrimination overlap our work. Our discrimination functions resemble those of Knill *et al.* (1990), particularly their low-contrast near condition (17.5% RMS



contrast at 1 meter with 64x64 pixel images), which is similar to our Far Sequential condition. While the average exponent of natural scenes is around 1.1 (Table 1), the greatest sensitivity to changes in a fractal image's exponent are consistently found to be around 1.6 across a wide range of conditions. We see no evidence for a second minimum at low  $\beta$  (circa 0.6) reported by Tadmor and Tolhurst, even when we used a simultaneous viewing condition similar to Tadmor and Tolhurst (1994). Nor is the discrepancy due to the angular size of the image, as all three studies had stimuli that were similar in size. Hansen & Hess (2006) note that the spatial presentation task uses two different parafoveal patches of retina, while the temporal task uses the same patch of central fovea; they find that fovea and parafovea yield somewhat different patterns of discriminability as a function of  $\beta$ , but none of their data show a second minimum at low  $\beta$  (rather, they find a maximum at  $\beta=0.8$ , with better thresholds on either side, similar to our findings). Another possible source of this difference in discriminability functions may be the specific nature of Tadmor and Tolhurst's task. In both the present study and Knill *et al.* (1990), standard two-Alternative Forced-Choice psychophysical procedures were used. In contrast, Tadmor and Tolhurst (1994) used an odd-one-out task (i.e., three images were presented simultaneously, two of which had identical exponents – the task was to choose the image that was different from the other two). In other words, Tadmor and Tolhurst's task was one of simple discrimination, while our task (and Knill's) requires discrimination and some form of identification (once the two images could be told apart, the subjects had to decide which had a lower exponent). These tasks coincide in difficulty only if all information required for identification is present at the discrimination threshold, which will most often take place when a single channel mediates performance of the task. Indeed, Tolhurst and Tadmor (1997) have shown that simple discrimination data is often consistent with a single channel mediating discrimination. However, since a comparison of channel outputs is required to estimate the spectral exponent of an image, discrimination plus identification would likely require a comparison of channel outputs, perhaps raising the JND for  $\beta$  near 0.4 sufficiently to eliminate the second minimum that Tadmor and Tolhurst (1994) found.



**Figure 5.** Camouflage can be dynamic in several ways, including simple movement. A Jordanian F-16 painted in HyperStealth Biotechnology Corp.'s fractal-like camouflage.

**Comparison to Related Studies: Dynamic Fractals**

So far we have discussed only perception of static fractals. But camouflaged images may move against their backgrounds and camouflage may be dynamic in other ways. In general, the effect of motion on such fractals is described by  $f_t = v * f_s$  (where  $v$  is velocity and  $f_t$  is temporal frequency). Thus, if the spatial spectrum is a  $1/f$  distribution, then for simple movement the temporal frequency distribution is a linear transform of spatial frequency, which is no more interesting than the viewing distance condition. There are however more interesting dynamic manipulations of fractals that are worth study. For example, it is possible to extend our study of discrimination to spatiotemporal fractals – fractals whose individual pixel intensities vary over time in a manner described by fractional Brownian motion. Such images have Fourier amplitude spectra of

$$A(f_t, f_s) = k f_t^{-\alpha} f_s^{-\beta} \tag{Eq. 2}$$

In general, as  $\alpha$  becomes larger, the motion of the texture becomes more coherent and can be used to mimic various biological motions (Billock et al., 2001a). Figure 6 shows the human perceptual discrimination space for spatiotemporal fractals (dynamic textures).

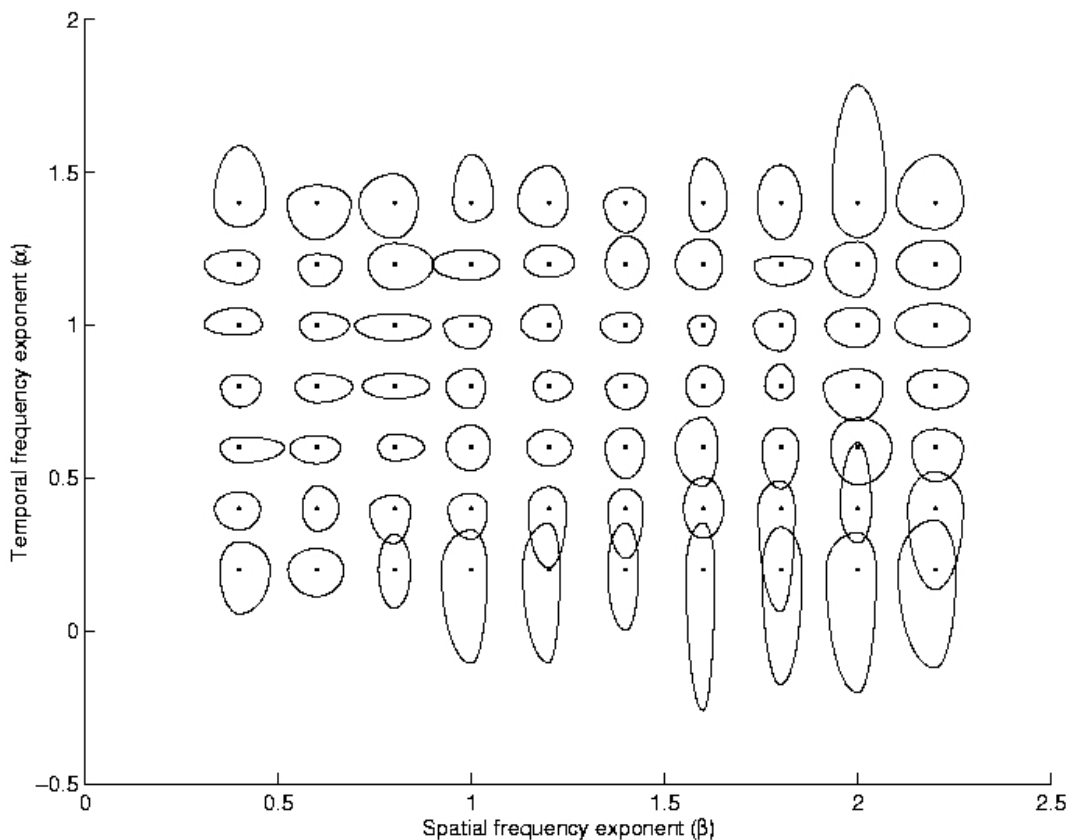


**Figure 6.** Discrimination contours for spatiotemporal fractal textures (Eq. 2) using the same observers in Figures 3 and 4. The contours are estimated using JNDs for discrimination in four directions in the perceptual space and are fit using simple quarter-circles of no theoretical significance.

To define two-dimensional JNDs we measured discrimination in four directions: both increments and decrements for both spatial ( $\beta$ ) and temporal ( $\alpha$ ) exponents. Not surprisingly, the JNDs in this space are ellipsoidal (they resemble color discrimination JNDs). Interestingly, the interior portion of the resulting two-dimensional discrimination space is remarkably flat, a feature that some psychophysicists have gone to great lengths to obtain in nonlinear mappings of other perceptual systems (e.g., color discrimination).

### ***Implications for Future Work***

It is worth noting that humans can become proficient at naming the spectral exponents of images (or equivalently, fractal dimension, which is a linear transform of the exponent; Cutting & Garvin, 1987; Kumar et al., 1993; Pentland, 1988). A neural ability to estimate the spectral drop-off and exploit it has been speculated on and deserves additional attention (Billock, 2000; Billock et al., 2001b; Campbell et al., 1978; Hammett & Bex, 1996; Rogowitz & Voss, 1990). Taken together with the natural image regularities and perceptual pop-out findings discussed earlier, this suggests that  $\beta$  is a key signature, both for images and for the visual systems that evolved to transduce images. Of particular interest is the finding that, under some conditions (nonlinear systems near threshold), adding noise can facilitate detection and identification of some signals, including images (Repperger et al., 2001; Simonotto et al., 1997; Yang, 1998) – an example of stochastic resonance as an image enhancement mechanism. Dynamic noise is more effective than static (Simonotto et al., 1997). Because other studies of stochastic resonance show that  $1/f^\beta$  noise can be more efficient than white noise in inducing stochastic resonance effects (Billock & Tsou, 2007; Hangi et al., 1993; Nozaki et al., 1999), further studies of discrimination in spatiotemporal fractal noise (at various contrast levels) would be warranted and might uncover some practical applications.

### ***Implications of Fractal Discrimination for Camouflage and Combat ID***

Based on this and other work we can enumerate some implications for camouflage and combat ID: (i) Natural images have  $1/f^\beta$  spatial amplitude spectra. The most reasonable value of  $\beta$  for general purpose camouflage is around 1.1. Particular environments will vary in this statistic and in coloration. (ii) Keeping the difference between the  $\beta_{\text{target}}$  and  $\beta_{\text{background}}$  less than 0.2 generally avoids preattentive popout, but discrimination will still be possible using a point-by-point search. (iii) Using many spatial scales makes camouflage effectiveness almost independent of distance. (iv) For IFF purposes, friendly camouflage schemes should have different  $\beta$ s than the unfriendly camouflage patterns, but this may conflict with concealment goals. The best outcome would be for hostile and friendly camouflage statistics to be on opposite sides of the  $\beta_{\text{background}}$  value, with the friendly scheme not easily discriminable from background but discriminable from the hostile. (v) For identification purposes, side-by-side viewing of sensor and reference images is preferable. Sensor operators should be screened for spatial sampling problems (sub-clinical amblyopia) by measuring their contrast sensitivity functions. (vi) It may be possible to break many camouflage schemes by adding filtered noise to the sensor images. This seemingly perverse aspect of stochastic resonance should be exploited if possible. Since stochastic resonance's effectiveness is often dependent on the Fourier spectral qualities of the noise, fractal camouflage may be particularly vulnerable (because the spectral qualities of simple fractals are easily matched by varying one noise parameter). Multi-fractals may be less vulnerable in this regard. It would be ironic if the beautiful mathematical attributes of fractals (which give it so

much utility in describing the natural environment and make it such an elegant solution to the problem of designing camouflage) also prove to be its Achilles' heel.

### **Author Note and Acknowledgements**

Vincent A. Billock, General Dynamics, Inc., Suite 200, 5200 Springfield Pike, Dayton, OH 45431; vince.billock@gd-ais.com. Douglas W. Cunningham, University of Tübingen, Tübingen, Germany; douglas.cunningham@gris.uni-tuebingen.de. Brian H. Tsou, AFRL/RHCI, Wright-Patterson Air Force Base, OH 45433; brian.tsou@afrl.af.mil. We thank Jer Sen Chen, Steven Fullenkamp, Paul Havig and Eric Heft for technical support.

## References

- Billock, V. A. (2000). Neural acclimation to 1/f spatial frequency spectra in natural images and human vision. *Physica D*, *137*, 379-391.
- Billock, V. A., Cunningham, D. W., Havig, P., & Tsou, B. H. (2001a). Perception of spatiotemporal random fractals: An extension of colorimetric methods to the study of dynamic texture. *Journal of the Optical Society of America A*, *18*, 2404-2413.
- Billock, V. A. de Guzman, G. C., & Kelso, J. A. S. (2001b). Fractal time and 1/f spectra in dynamic images and human vision. *Physica D*, *148*, 136-146.
- Billock, V. A., & Tsou, B. H. (2007). Neural interactions between flicker-induced self-organized visual hallucinations and physical stimuli. *Proceedings of the National Academy of Sciences USA*, *104*, 8490-8495.
- Billock, V. A., Vingrys, A. J., & King-Smith, P. E. (1994). Opponent-color detection threshold asymmetries may result from reduction of ganglion cell subpopulations. *Visual Neuroscience*, *11*, 99-109.
- Burton, G. J., & Morehead, I. R. (1987). Color and spatial structure in natural scenes. *Applied Optics*, *26*, 157-170.
- Caelli, T. (1981). *Visual Perception: Theory and Practice*. Oxford: Pergamon Press.
- Campbell, F. W., Howell, E. R., & Johnson, J. R. (1978). A comparison of threshold and suprathreshold appearance of gratings with components in the low and high spatial frequency range. *Journal of Physiology*, *284*, 193-201.
- Cutting, J. E., & Garvin, J. J. (1987). Fractal curves and complexity. *Perception and Psychophysics*, *42*, 365-370.
- Dong, D. W., & Atick, J. J. (1995). Statistics of time-varying images. *Network: Computation in Neural Systems*, *6*, 345-358.
- Field, D. J. (1987). Relations between the statistics of natural images and the response properties of cortical cells. *Journal of the Optical Society of America A*, *4*, 2379-2394.
- Field, D. J. (1993). Scale invariance and self-similar wavelet transforms: An analysis of natural scenes and mammalian visual systems, in M. Farge, J. C. R. Hunt, & J. C. Vassilicos (Eds.), *Wavelets, Fractals and Fourier Transforms* (pp. 151-193). Oxford: Clarendon Press.
- Field, D. J., & Brady, N. (1997). Visual sensitivity, blur and the sources of variability in the amplitude spectra of natural images. *Vision Research*, *37*, 3367-3383.
- Garcia-Perez, M. A., Giorgi, R. G., Woods, R. L., & Peli, E. (2005). Thresholds vary between spatial and temporal forced-choice paradigms: The case of lateral interactions in peripheral vision. *Spatial Vision*, *18*, 99-127.
- Hammett, S. T., & Bex, P. J. (1996) Motion sharpening: Evidence for addition of high spatial frequencies to the effective neural image. *Vision Research*, *36*, 2729-2733.
- Hangi, P., Jung, P., Zerbe, C., & Moss, F. (1993). Can colored noise improve stochastic resonance? *Journal of Statistical Physics*, *70*, 25-47.
- Hansen, B. C., & Hess, R. F. (2006). Discrimination of amplitude spectrum slope in the fovea and parafovea and the local amplitude distributions of natural scene imagery. *Journal of Vision*, *6*, 696-711.
- van Hateren, J. H. (1992). Theoretical predictions of spatiotemporal receptive fields. *Journal of Comparative Physiology A*, *171*, 151-170.

- Julesz, B. & Caelli, T. (1979). On the limits of Fourier decompositions in visual texture perception. *Perception*, 8, 69-73.
- Knill, D. C., Field, D., & Kersten, D. (1990). Human discrimination of fractal images. *Journal of the Optical Society of America A*, 7, 1113-1123.
- Kumar, T., Zhou, P., & Glaser, D. A. (1993). A comparison of human performance with algorithms for estimating fractal dimension of fractional Brownian statistics. *Journal of the Optical Society of America A*, 10, 1136-1146.
- MacMillan, N. A., & Creelman, C. D. (1991). *Detection Theory: A User's Guide*. Cambridge: Cambridge University Press.
- Moulden, B., Kingdom, F., & Gatley, L. F. (1990). The standard deviation of luminance as a metric for contrast in random-dot images. *Perception*, 19, 79-101.
- Nozaki, D., Collins, J. J., & Yamamoto, Y. (1999). Mechanism of stochastic resonance enhancement in neuronal models driven by 1/f noise. *Physical Review E*, 60, 4637-4644.
- O'Neill, T., Matthews, M., & Swiergosz, M. (2004). Marine Corps innovative camouflage. *Midyear meeting of the American Psychological Association, Divisions 19 & 21*. Supplementary data at <http://www.hyperstealth.com/digital-design/index.htm>
- Parraga, C. A., Brelstaff, G., Troscianko, T., & Morehead, I. R. (1998). Color and luminance information in natural images. *Journal of the Optical Society of America A*, 15, 563-569.
- Parraga, C. A., & Tolhurst, D. J. (2000). The effect of contrast randomization on the discrimination of changes in the slopes of the amplitude spectra of natural scenes. *Perception*, 29, 1101-1116.
- Peli, E. (1990). Contrast in complex images. *Journal of the Optical Society of America A*, 7, 2032-2040.
- Peli, E. (1997). In search of a contrast metric: matching the perceived contrast of Gabor patches at different phases and bandwidths. *Vision Research*, 23, 3217-3224.
- Pentland, A. (1988). Fractal-based descriptions of surfaces, in W. Richards (Ed.), *Natural Computation* (pp. 279-299). Cambridge: MIT Press.
- Repperger, D. W., Phyllips, C. A., Neidhard, A., & Haas, M. (2001). Designing human machine interfaces using principles of stochastic resonance. *AFRL Technical Report ARRL-HE-WP-TR-2002-0187*. DTIC# ADA412330.
- Rogowitz, B. E., & Voss, R. F. (1990). Shape perception and low-dimension fractal boundaries. *Proceedings of the SPIE*, 1249, 387-394.
- Ruderman, D. L. (1994). The statistics of natural images. *Network: Computation in Neural Systems*, 5, 517-548.
- van der Schaaf, A., & van Hateren, J. H. (1996). Modeling the power spectra of natural images: statistics and information. *Vision Research*, 36, 2759-2770.
- Simonotto, E., Riani, M., Seife, C., Roberts, M., Twitty, J., & Moss, F. (1997). Visual perception of stochastic resonance. *Physical Review Letters*, 78, 1186-1189.
- Tadmor, Y., & Tolhurst, D. J. (1994). Discrimination of changes in the second-order statistics of natural and synthetic images. *Vision Research*, 34, 541-554.
- Taylor, R. P., Spahar, B., Wise, J. A., Clifford, C. W. G., Newell, B. R., & Martin, T. P. (2005). Perceptual and physiological responses to the visual complexity of fractal patterns. *Nonlinear Dynamics in Psychology and Life Sciences*, 9, 89-114.
- Thomson, M. G. A., & Foster, D. H. (1997). Role of second- and third-order statistics in the discriminability of natural images. *Journal of the Optical Society of America A*, 14, 2081-2090.

- Tolhurst, D. J., & Tadmor, Y. (2000). Discrimination of spectrally blended natural images: Optimization of the human visual system for encoding natural images. *Perception, 29*, 1087-1100.
- Tolhurst, D. J., & Tadmor, Y. (1997). Band-limited contrast in natural images explains the detectability of changes in the amplitude spectra. *Vision Research, 23*, 3203-3215.
- Tolhurst, D. J., Tadmor, Y., & Chao, T. (1992). The amplitude spectra of natural images. *Ophthalmic and Physiological Optics, 12*, 229-232.
- Webster, M. A., & Miyahara, E. (1997). Contrast adaptation and the spatial structure of natural images. *Journal of the Optical Society of America A, 14*, 2355-2366.
- Voss, R.F. (1985). Random fractal forgeries, in R.A. Earnshaw, Ed., *Fundamental Algorithms for Computer Graphics* (pp. 805-835). Berlin: Springer.
- Yang, T. (1998). Adaptively optimizing stochastic resonance in visual system. *Physics Letters A, 245*, 79-86.